

ASSESSING DISEASE SEVERITY OF RICE BACTERIAL LEAF BLIGHT WITH CANOPY HYPERSPECTRAL REFLECTANCE

Chwen-Ming Yang^{1*} and Yih-Chang Chang²

¹ Senior Agronomist/Research Fellow, Crop Science Division, Taiwan Agricultural Research Institute, Taichung Hsien 41301, Taiwan ROC; Phone: +886-4-2330-2301 ext.135, Fax: +886-4-2339-6057, E-mail: cmyang@wufeng.tari.gov.tw

² Plant Pathologist/Associate Research Fellow, Plant Pathology Division, Taiwan Agricultural Research Institute, Taichung Hsien 41301, Taiwan ROC

KEY WORDS: Canopy hyperspectral reflectance, Spectral model, Disease severity assessment, Rice bacterial leaf blight, Spectral characteristics

ABSTRACT: The bacterial leaf blight [*Xanthomonas oryzae* pv. *oryzae* (ex Ishiyama); BLB] is an important vascular disease to irrigated rice and may cause significant yield reduction under serious infestations. This study was to hyperspectral analyses near-ground canopy reflectance spectra of two rice (*Oryza sativa* L.) cultivars with different disease susceptibilities so as to establish spectral models to assess disease severity for applications in site-specific management. By simple linear correlation analysis between spectral reflectance and infestation fractions, the highest absolute value of correlation coefficient (r) was found located at 943 nm ($r_{\max} = -0.908^{**}$) for the moderate susceptible cultivar TNG 67. For the high susceptible cultivar TCS 10, r_{\max} located at 745 nm (-0.959^{***}). The first derivative values in range of 640-1050 nm had a peak near 708 nm for TNG 67 and 726 nm for TCS 10, which corresponded to the turning point of red edge shoulder, and the derivative values ($dR/d\lambda \big|_{708 \text{ nm}}$ and $dR/d\lambda \big|_{726 \text{ nm}}$) correlated linearly with fractions of infested area. All the calculated spectral indices (SIs) had significant relationships with fractions of infested area in cultivar TCS 10, while only $R_{\text{NIR}} - R_{\text{RED}}$ ($R^2 = 0.873$, $P < 0.001$) and red edge slope ($R^2 = 0.842$, $P = 0.004$) correlated significantly with infestation fractions in cultivar TNG 67, where R_{NIR} was the reflectance at near infrared peak (NIR) and R_{RED} was the reflectance at chlorophyll absorption maximum (RED). The disease severity assessment on the spectral reflectance in cultivar TNG 67 was further improved by using the multiple linear regression (MLR) approach. The best two-variable MLR equation incorporating characteristic narrow bands of 943 nm and 1039 nm increased R^2 to 0.889 ($P < 0.0001$), providing a greater sensitivity to phenological variation of blight-infested plants.

1. INTRODUCTION

Rice (*Oryza sativa* L.) is the primary food source for more than three billions people, and is also one of the world's most important staple crops, second only to wheat and corn. However, a significant amount of the potential yield of the world rice crop is lost each year to diseases caused by bacteria, fungi and viruses. In Taiwan, leaf blast (*Pyricularia oryzae* Cav.), bacterial leaf blight (BLB) and sheath blight (*Thanatephorus cucumeris* (Frank) Donk; or *Rhizoctonia solani* Kuhn) have been ranked the three top most serious diseases in irrigated rice. Among them BLB occurs in both first and second cropping seasons locally, and is considered a potential threat to rice production. Symptoms of leaf wilting and rolling appear in rice seedlings infected by the pathogen, and leaf color turns grayish-green to yellow as the disease progress until the

whole seedling dies. In mature rice plants, lesions begin as water-soaked stripes on the leaf blades and would expand in size becoming yellow to grayish-white until the entire leaf dries up. Under serious infestation conditions, it may cause severe yield losses. Thus, estimating the occurrence of this disease and the subsequent use of the derived information to facilitate timely controlling practices are critical to avoid significant production losses.

Disease control can be more efficient if the spatial and temporal distribution of disease incidence within fields could be identified and specified. Recent developments in spectral remote sensing technology have the potential to enable direct detection and assessment of foliar symptoms caused by diseases and pests under field conditions so that suitable amounts of chemical spray could be timely applied in a site-specific way only to the infested areas. Reflectance of agriculture crops in the visible and infrared regions has been studied in order to estimate different crop parameters and assess crop growth status. In conditions in favor of photosynthetic activity, generally most crop canopies exhibit a spectral reflectance profile of higher reflectance in near-infrared region (700-1300 nm; Nir) and lower reflectance in the photosynthetically active region (400-700 nm; PAR) (Hall et al., 2002). Under pest infestation conditions, a decrease in plant vigor and canopy coverage related to Nir and an increase in the chlorophyll absorption related to PAR were commonly observed (Knipling, 1970; Yang and Chen, 2004; Yang et al., 2007). Decreases in leaf area and foliage density and changes in leaf orientation and canopy architecture caused by necrosis, discoloration and leaf breakdown would lower down the values of Nir reflectance while elevate PAR reflectance. Apparently there is potential in using spectral reflectance measurements for quantifying the incidence or severity of plant diseases. It is also possible to estimate the severity of disease based on disease prevalence (fraction of infested area). Such information can help in the analysis of the level of disease development and be further used to the assessment of applicable strategies for management practices, especially in areas prone to disease outbreaks.

The in-situ spectral reflectance measurements of rice canopy infested with BLB were taken and used to study alterations in optical properties to disease infestations. By using two cultivars with varied disease susceptibility, changes in spectral characteristics (SCs) to the intensity of BLB were examined, reflectance variations in different wavebands were compared, and the regression models suitable for assessing infestation severity were developed and validated.

2. MATERIALS AND METHODS

2.1 Rice Cultivation and Bacterial Inoculations

Field experiments were conducted in the second cropping seasons of 2001 and 2005 at the Taiwan Agricultural Research Institute Experimental Farm, Taiwan (24°45' N, 120°54' E, 85 m above sea level). Seedlings were machine transplanted to north-south rows with hill distance of 0.30 m × 0.18 m resulting in a population density of 1.85×10^5 hills ha⁻¹. The transplanting date was on August 3 and the harvest date was on November 26 in 2001, while seedlings were transplanted on August 4 and grains were harvested on November 25 in 2005. Plants were prevented from the infestations of insects, snails and weeds by applying pesticides and herbicides recommended by local authority. Two semi-dwarf rice cultivars of varied BLB susceptibility and growth types were chosen. Cultivar TNG 67, a *japonica* type with moderate

susceptibility to BLB, was grown in 2001. Cultivar TCS 10, an *indica* type with high susceptibility, was grown in 2005. Leaves were inoculated by clipping off leaf tips with scissors that had been dipped in bacterial suspension. Attempts had been made to create distinct disease epidemics by varying the time and the numbers of inoculations.

2.2 Infestations Labeling and Spectral Measurements

A visual inspection of disease severity, i.e., fraction of infested area, was taken periodically following bacterial inoculations. Symptoms of blight lesions giving striped appearance elongated over the leaves so that fractions of infested area can be visually estimated. Measurements of canopy high-resolution reflectance spectra were performed on two consecutive days, October 23-24 in 2001 and October 20-21 in 2005, in the early stage of grain filling where rice crop reached more than 90% canopy cover based on visual estimates. Groups of rice hills infested with varied levels of BLB were identified from inoculated field plots, with fractions of infested area in one square meter ranged from 6 to 19% in 2001 (9 levels) and 0.5 to 55% in 2005 (14 levels), and hyperspectral reflectance from the targeted areas was measured individually. The reflectance of the healthy hills from the field plot not treated with the pathogen was also taken to spectrally characterize the healthy check (0%; CK).

The operating system for spectral measurements consists of a field portable spectroradiometer (model GER-2600, Geophysical & Environmental Research Corp., NY, USA), a 10 degrees field-of-view (FOV) lens, a notebook computer, batteries, and cables. The two-spectrometer radiometer operates in a range from 330 to 2600 nm, while only reflectance data in the range of 350-2500 nm were used to avoid severe noise in both ends of the spectrum reduced spectral channels to 573. Spectral measurements and calibrations are controlled by simple menu-driven software supplied by GER on the computer. The in-situ canopy spectral reflectance measurements were acquired at the time as the disease inspections were carried out. The system unit was mounted on a 4 wheel-drive adjustable mobile lift raised 2.9 m vertically above the rice canopy surface, resulting in a sampled area ca. 0.5 m in diameter, pointing downwards in a nadir viewing to measure canopy radiance. Each measurement of radiance spectrum from targeted areas was the average of four consecutive full spectral range scans, took less than four seconds per data set. Target measurements were collected immediately after the reference measurements, which were taken from a spectral reference panel (99% 'Spectralon' panel, Labsphere, Inc., North Sutton, NH, USA) of known spectral characteristics to compute reflectance spectrum. About five to ten spectra were recorded from random target regions on each level during the two sampling days, and the mean spectral curve of each level was calculated from pooled data and used in the statistical analyses. All spectral data were collected under near cloud-free conditions between 10:00 to 13:00 local time to minimize the effect of changes in zenith angle.

2.3 Data analyses and Statistics

Spectral data collected from this study were analyzed and graphed by using the software packages Statistical Analysis System version 8.1 and Sigmaplot 2001 (SPSS ASC BV, the Netherlands). Three distinct locations of reflectance spectra, that is, narrow band at the chlorophyll absorption minimum (GREEN) of the green light (490–560 nm), narrow band at the chlorophyll absorption maximum (RED) of the red light (640–740 nm), and narrow band at the peak (NIR) of the near-infrared (740–1300 nm), were identified dynamically from each of the spectra to calculate

the spectral indices (SIs). In addition to $R_{NIR} - R_{RED}$, $R_{NIR} + R_{RED}$ and $\lambda_{NIR} - \lambda_{RED}$, ratio-based SIs R_{RED}/R_{NIR} ratio, R_{NIR}/R_{GREEN} ratio, R_{RED}/R_{GREEN} ratio, normalized difference vegetation index (NDVI) and red edge slope (RES) were also calculated. The NDVI and RES were determined by the formulae: $NDVI = (R_{NIR} - R_{RED})/(R_{NIR} + R_{RED})$ and $RES = (R_{NIR} - R_{RED})/(\lambda_{NIR} - \lambda_{RED})$, respectively. For accuracy assessment, mean bias error (MBE) and root mean square error (RMSE) were calculated.

3. RESULTS AND DISCUSSION

As leaf blade appears wavy margins and gradually dries-up as the disease progress, changes in leaf coloration and appearance caused by varied levels of disease severity of LBL reflected in the variation of the acquired canopy reflectance spectra as expected. By simple linear correlation analysis between spectral reflectance and infestation fractions, results showed that wavebands ranged from 757 nm to 1039 nm was the most sensitive region and the highest absolute value of correlation coefficient (r) located at 943 nm ($r_{max} = -0.908^{**}$) for the moderate susceptible cultivar TNG 67, yet reflectance distribution was better displayed in a quadratic correlation ($R^2 = 0.858$, $P = 0.003$) (Figure 1). For the high susceptible cultivar TCS 10, most narrow bands showed a significant relationship and r_{max} located at 745 nm (-0.959^{***}) with reflectance distributed in a curvilinear function ($R^2 = 0.964$, $P < 0.001$) (Figure 1). As the results indicated, changes in reflectance of rice canopy upon disease incidence were waveband-dependent and severity-sensitive, and reflectance in the Nir was the region most responsive to infestations of BLB. Apparently an alteration of internal tissue structure and/or plant vigor must have occurred in plant population infested with BLB, and thus resulted in a substantial reduction of canopy reflectance in Nir region. The chlorophyll-related activities and tissues moisture content may also affected by the infestations of the bacterium as reflectance varied in PAR and shortwave infrared and mid-infrared wavebands.

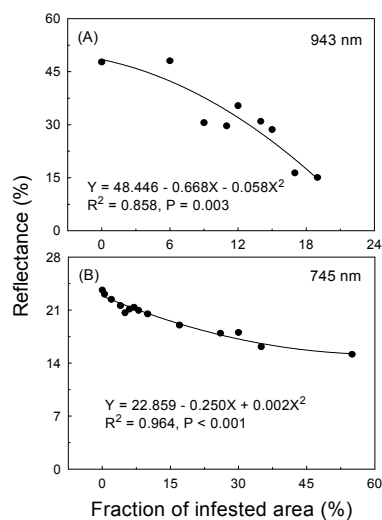


Figure 1. The correlation between values of reflectance at (A) 943 nm (rice cultivar TNG 67) and (B) 745 nm (rice cultivar TCS 10) and fractions of infested area caused by bacterial leaf blight infestations for rice plants grown in early stage of grain-filling of the second growing season in 2001 and 2005, respectively.

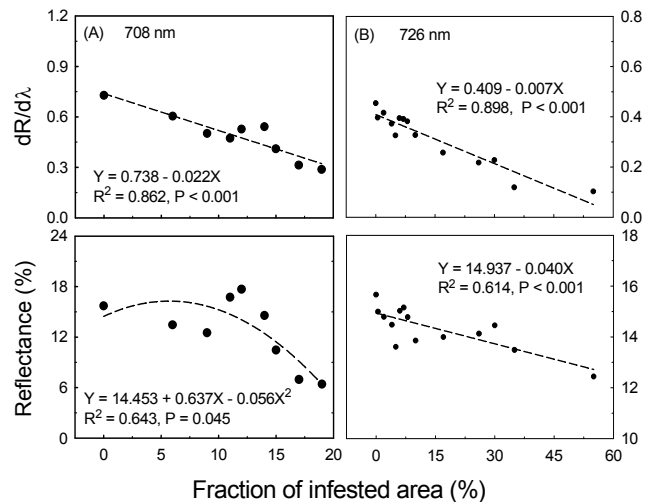


Figure 2. Correlations between the values of first order derivative and the values of reflectance at red edge shoulder turning points, (A) 708 nm (rice cultivar TNG 67) and (B) 726 nm (rice cultivar TCS 10), and fractions of infested area, caused by bacterial leaf blight infestations for rice plants grown in early stage of grain-filling of the second growing season in 2001 and 2005, respectively.

With the first order differentiation calculations, the first order derivative values ($dR/d\lambda$) of canopy reflectance spectrum along spectral axis for each infestation level were obtained. The first peak in range 640-1050 nm, which corresponded to the turning point of red edge shoulder, was identified locating around 708 nm in TNG 67 and 726 nm in TCS 10 for all levels of infestation. Their derivative values ($dR/d\lambda|_{708\text{ nm}}$ and $dR/d\lambda|_{726\text{ nm}}$) with fractions of infested area were a linear correlation ($R^2 = 0.862$ and $P < 0.001$ for TNG 67; $R^2 = 0.898$ and $P < 0.001$ for TCS 10), and the correlations were stronger than their reflectance values ($R^2 = 0.643$ and $P = 0.045$ for TNG 67; $R^2 = 0.614$ and $P < 0.001$ for TCS 10) (Figure 2). As red edge refers to the region of rapid change in reflectance of chlorophyll in the Nir, a decrease in values of $dR/d\lambda|_{708\text{ nm}}$ or $dR/d\lambda|_{726\text{ nm}}$ following the increase of disease severity accounts for a reduction of foliage brightness and an alleviation of photosynthesis.

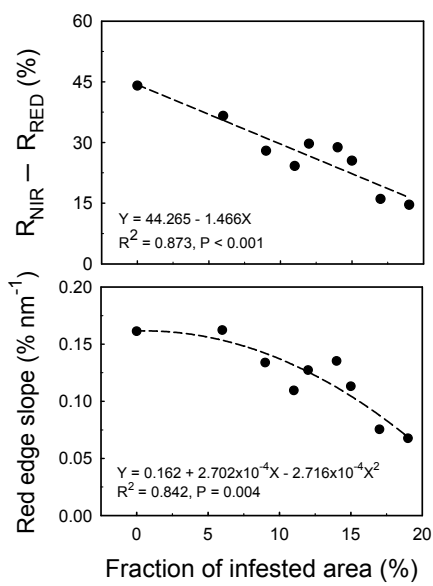


Figure 3A. Correlations between spectral indices $R_{NIR} - R_{RED}$ and red edge slope and fractions of infested area caused by bacterial leaf blight infestations for rice plants (cultivar TNG 67) grown in early stage of grain-filling of the second growing season in 2001.

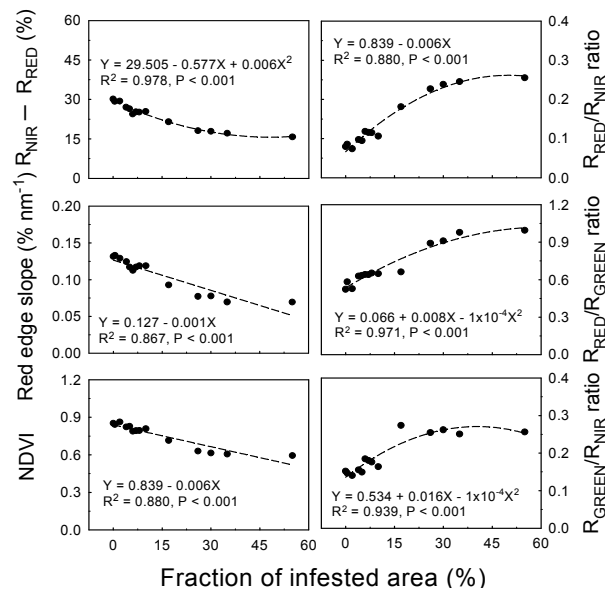


Figure 3B. Correlations between spectral indices $R_{NIR} - R_{RED}$, red edge slope, NDVI, R_{RED}/R_{NIR} ratio, R_{RED}/R_{GREEN} ratio and R_{GREEN}/R_{NIR} ratio and fractions of infested area caused by bacterial leaf blight infestations for rice plants (cultivar TCS 10) grown in early stage of grain-filling of the second growing season in 2005.

Within the SIs calculated with two SCs, only $R_{NIR} - R_{RED}$ and RES correlated significantly with infestation severity in TNG 67 (Figure 3A). It was a negative linear relationship for $R_{NIR} - R_{RED}$ ($R^2 = 0.973$, $P < 0.001$) and a negative quadratic function for RES ($R^2 = 0.842$, $P = 0.004$). Comparing with the results of single SC, R^2 was slightly improved from 0.862 of $dR/d\lambda|_{708\text{ nm}}$ to 0.873 of $R_{NIR} - R_{RED}$. On the other hand, all calculated SIs had significant relationships with fractions of infested area in high susceptible cultivar TCS 10, and $R_{NIR} - R_{RED}$ again obtained the highest R^2 value (0.978) (Figure 3B). Apparently infestations of BLB would affect factors involved in pigment absorption (responsive to R_{RED}) and vegetation coverage (responsive to R_{NIR}) irrespective to disease severity, as in case of brown planthopper infestations (Yang et al., 2007), and varietal susceptibility.

The influence of blight infestations on the spectral reflectance was further evaluated by using the MLR approach for severity assessment improvement in the moderate susceptible cultivar TNG 67. Reflectance of seven narrow bands from the measured spectral domain of each infestation levels were selected and used as inputs for MLR analysis. The best two-variable MLR equation established for estimation of fraction of infested area by BLB was obtained (data not shown), and the value of R^2 was further improved to 0.889 ($P < 0.0001$). With the MLR approach, characteristic narrow bands (943 nm and 1039 nm) for a better estimation function were developed, which provided a greater sensitivity to phenological variation of blight-infested plants and improved the models' ability to assess BLB infestations. Validation of measured and model estimated values of fractions of infested area using another set of spectral data of different severity levels was made (Figure 4). The relationship was significantly correlated linearly ($r = 0.938^{**}$) with the slope of 0.855, MBE of 0.584, and RMSE of 2.004. Results suggest that the MLR equation developed from this study could be applied for estimating/assessing disease severity of less susceptible rice cultivars and the spectral model produced following this procedure could be used in studying and monitoring spectral remote sensing for disease infestations assessment.

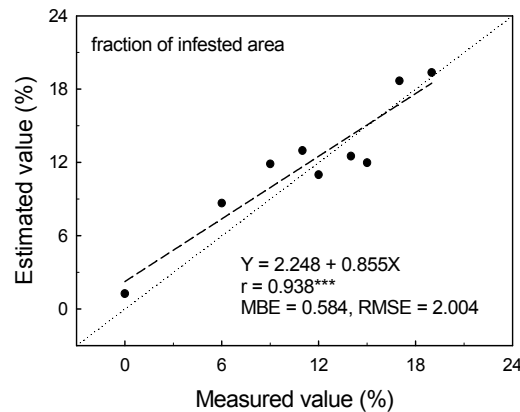


Figure 4. Comparison between the estimated values from multiple linear regression model and the measured values of fraction of infested area caused by bacterial leaf blight infestations for rice plants (cultivar TNG 67) grown in early stage of grain-filling of the second growing season in 2001.

5. REFERENCES

- Hall, A., Lamb, D.W., Holzapfel, B., & Louis, J., 2002. Optical remote sensing applications for viticulture—a review. *Australian Journal of Grape and Wine Research*, 8, pp. 36–47
- Knippling, E.B., 1970. Physical and physiological basis for differences in reflectance of visible and near-infrared radiation from vegetation. *Remote Sensing of Environment*, 1, pp. 155–159
- Yang, C.-M., & Chen, R.-K., 2004. Modeling rice growth using hyperspectral reflectance data. *Crop Science*, 44, pp. 1283-1290
- Yang, C.-M., Cheng, C.-H., & Chen, R.-K., 2007. Changes in spectral characteristics of rice canopy infested by leaf folder and brown planthopper. *Crop Science*, 47, pp. 329-335